# Planning of Hybrid AC-DC Microgrid with High Penetration of Renewable Energy Sources

Muhammad Baseer[1], Geev Mokryani[1], Rana.H.A.Zubo[1], Steve Cox[2],
[1] University of Bradford, Bradford BD7 1DP, UK
[2] Electricity north west limited, UK
Emails: {m.baseer, g.mokryani,r.h.a.zubo}@bradford.ac.uk[1], Steve.cox@enwl.co.uk[2]}

**Abstract: - Hybrid AC-DC microgrid (HMG) allows direct integration of both AC distributed generators (DGs) and DC DGs, AC and DC loads into the grid. The AC and DC sources, loads are separate out and are connected to respective subgrid mainly to reduce the power conversion, thus the overall efficiency of the system increases. This paper aims to introduce a novel hybrid AC-DC microgrid planning and design model within a microgrid market environment to maximize net social welfare (NSW). NSW is defined as present value of total demand payment minus present value of total planning cost including investment cost of distributed energy sources (DERs) and converters, operation cost of DERs and the cost of energy exchange with the utility grid subject to network constraints. Scenario Tree approach is used to model the uncertainties related to load demand, wind speed and solar irradiation. The effectiveness of the proposed model is validated through the simulation studies on a 28-bus real hybrid AC-DC microgrid.**

**keywords-** Interlinking converter, distributed generator, hybrid microgrid, net social welfare, distributed energy sources.

Nomenclature

Indices

| | |
|---|---|
| $y$ | Index for year |
| $h$ | Index for buses |
| $s$ | Index for scenarios |
| $nh$ | Index for number of hours |

Sets

| | |
|---|---|
| $a$ | Set of all DGs |
| $i$ | Set of DC DGs |
| $k$ | Set of AC DGs |

Parameters

| | |
|---|---|
| $C_{AC}$ | Generation price for AC DGs |
| $C_{DC}$ | Generation price for DC DGs |
| $CC_{a}$ | Annualized investment cost of DGs |
| $CR$ | Annualized investment cost of ac to dc rectifier |
| $CI$ | Annualized investment cost of dc to ac inverter |
| $R$ | Discount rate |
| $P^{Limit}$ | Flow limits between utility grid and microgrid |
| $RR$ | Capital recovery rate |
| $ER$ | Rectifier efficiency |
| $EI$ | Inverter efficiency |
| $\rho$ | Market price |

Variables

| | |
|---|---|
| IC | Investment cost |
| OMG | Operation and maintenance cost |
| $P^{Max}$ | Installed DGs capacity |
| $P^{Fexch}$ | Power exchange at bus |
| $P^{Gexch}$ | Power exchange with grid |
| $W$ | Binary decision variable for dc bus |
| $f$ | Binary decision variable for the connection of DG with bus |
| $d$ | Binary decision variable for bus state |

## 1. Background, Motivation and Literature Review

The demand of electricity is increasing which necessitates more penetration from the generating units and an efficient power grid operation [1]. Population increase, good living standards, pollution, decrease in production of traditional energy resources like (natural gas, petroleum, coal etc.) are the main contributors of present critical situation. There are many disadvantages of fossil fuel like emission of gases which causes global warming and pollution [2]. The arrival of the Climate Change Act in 2008 and the subsequent rollout of electricity market reforms saw the United Kingdom (UK) become a world leader in renewables, particularly wind power [3]. To meet these targets, the UK government has set five-yearly carbon budgets which currently run until 2032. They restrict the amount of greenhouse gas the UK can legally emit in a five year period [5].

Microgrids are considered as a future of distribution system [5]. In Microgrids, a local grouping of energy generating sources and loads is formed which is able to feed its localized demand hence improves efficiency of the grid. In microgrid concept, there is a reduction in multiple reverse connections in an individual AC or DC grid but it also facilitates renewable AC-DC sources and loads to connect with the power system [6]. Although the AC power systems from the last few decades have improved a lot but the development in power electronics have completely revolutionized the major domains of power system and completely changed the load profile for end users. The modern appliances like laptops, mobiles, electric vehicles, TV, remote controllers, etc. operates on DC supply mostly fed through AC-DC converter [7]. Integration of DC technology into the existing system needs a smooth process. Especially, hybrid AC-DC microgrids can facilitate the DC power integration into existing AC system [8].

Hybrid microgrids can benefits both AC and DC microgrid types. Moreover, there would be a huge reduction in the number of required power converters which would enhance the microgrid efficiency and reduce investment and operation costs [9]. The prior research so far on hybrid AC-DC microgrid planning is limited and only few literatures can be found on modeling of individual DC or AC microgrid planning. In Ref. [10], different aspects of ac and dc microgrids were discussed. A planning model was developed which determines optimized DG generation mix and the type of microgrid, i.e., ac or dc. In Ref. [11], an inclusive review on technologies used in AC and DC microgrid is provided and different parameters, topographies, merits and demerits of each technology are discussed. It is described that DC microgrid has more advantages over AC microgrid especially for longer distances. For example, DC lines exhibits less line losses and more transmittable power. Conversely DC protection system is more expensive as compare to AC protection system. The standardization and islanding control techniques of DC systems needs more research. It is suggested at the end that hybrid microgrid could be more viable solution than DC microgrids. In Ref. [12], a decentralized multiagent-based real-time control model of hybrid microgrid is proposed without considering uncertainties. In Ref. [13], the uncertainties in microgrid are studied. In Ref. [14], dynamic assessment for hybrid microgrid is studied. In Ref. [15], different sources of uncertainties are studied. The planning solution for microgrid is divided into an investment and operation sub problems. In Ref. [16], a coordinated real time control algorithm of hybrid AC-DC microgrid's sources is presented and simulation results are validated with experimental results. In Ref. [17], authors proposed energy management and operational modeling of hybrid microgrid. They studied the optimal operation of hybrid microgrid by investigating the time dependence impacts on the network over the period of 24 h. In Ref. [18], it is presented that the hybrid microgrid can provide reliability to customer's nodes by appropriate DG allocation considering its size, location and type. In Ref. [19], a microgrid planning objective is to determine optimal size and type of DG that is to be installed having the mixture of heat and power systems is investigated. In Ref. [20], authors presents a hybrid microgrid which can integrate different small-size DGs into existing power system. A decoupled control model for hybrid microgrid is developed and its performance is analysed. In Ref. [21], the integration of DGs in hybrid microgrids model is proposed. Additional dc line is assumed at the connection point of DGs. In Ref. [22], planning of hybrid AC-DC is discussed. In Ref. [23], a comprehensive review of control strategies is given focusing on modeling, power management and control, stability, protection strategies and power quality. In the end, research gaps are identified and possible solutions are proposed.

The existing studies lack planning of hybrid AC-DC microgrid under uncertainties as most of the research is mainly focused on operation of HMG. Authors in Ref.[11-14] and [16-21] has discussed operation of microgrid while authors in [15] discussed planning of AC microgrid. Authors in [13,15] discussed uncertainty modeling in AC microgrids. Comparison of the existing studies and the proposed model is shown in Table 1. To the best of Authors knowledge, there is no literature available that considers the planning of HMG within the electricity market. This paper proposes a novel approach for planning of hybrid AC-DC microgrid within a novel microgrid market environment by maximizing net social welfare (NSW) considering uncertainties associated with DERs and dispatchable load demand.

**Table 1.** Proposed model comparison with existing ones.

| Reference | Microgrid Type | Planning | Uncertainty modeling | Power market |
|---|---|---|---|---|
| [11] | Hybrid AC-DC | No | No | No |
| [12] | Hybrid AC-DC | No | No | No |
| [13] | AC Microgrid | No | Yes | No |
| [14] | Hybrid AC-DC | No | No | No |
| [15] | AC | Yes | Yes | No |
| [16-21] | Hybrid AC-DC | No | No | No |
| [22] | Hybrid AC-DC | Yes | No | No |
| **Proposed** | **Hybrid AC-DC microgrid** | **Yes** | **Yes** | **Yes** |

The rest of the paper is organized as follows. Section 2 presents author's aim and approach. Section 3 includes the study related to uncertainties associated with wind speed and solar irradiations Section 4 presents planning and design of hybrid AC-DC microgrid. Section 5 presents hybrid microgrid electricity model. Section 6 includes a case study for a test microgrid and discussion on the proposed model results and finally conclusions are provided in section 7.

## 2. Aim and approach

It is evident that the prior work on microgrid planning is very limited and to the best of authors' knowledge there is no literature available regarding the planning and design of hybrid AC-DC microgrid within a market environment considering uncertainties and power flow of interlinking converters. This paper proposes a novel approach for planning of hybrid AC-DC microgrid within a novel microgrid market environment by maximizing NSW considering uncertainties associated with DGs and dispatchable load demand subject to network constraints and power flow of interlinking converters. Scenario Tree approach is used to model the uncertainties related to load demand, wind speed and solar irradiation. The method evaluates the optimal amount of active power generated by WT and PV over the planning horizon.

## 3. Uncertainty Modelling

### 3.1 Wind speed modeling

The wind speed variation modeling is done using Weibull PDF [24-27]. The PDF function that gives relationship between the speed of wind and the output power of WTs is given by [28].

$$PDF(v) = (\frac{k}{c})(\frac{v}{c})^{k-1} \exp\left[-(\frac{v}{c})^k\right] \tag{1}$$

where $v$ represents speed of wind, $c$ is the Weibull PDF scale index and $k$ represents the shape index. The WT's generated power can be evaluated by using its power curve as follows [29, 30]:

$$P_w(v) = \begin{cases} 0, & 0 \le v \le v_{ci} \\ P_{rated} \times \dfrac{v - v_{ci}}{v_r - v_{ci}}, & v_{ci} \le v \le v_r \\ P_{rated}, & v_r \le v \le v_{co} \\ 0, & v_{co} \le v \end{cases} \tag{2}$$

where $P_w$ is WTs generated power, $P_{rated}$ represents the rated power, $v_{ci}$ represents the cut-in speed, rated speed of WTs is represented by $v_r$ and $v_{co}$ is cut-off speed. The WTs Speed power curve is shown in Fig 1.

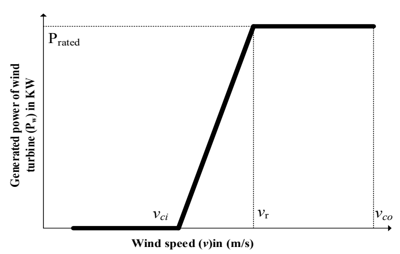

***Fig.1***. *WTs Speed power curve.*

At the bus $i$ and for scenario $s$, the active wind power is calculated as follows:

$$0 \le P_{i,s}^{w} \le \gamma_{i,s}^{w} \times P_{i,rated}^{w} \tag{3}$$

where $\gamma_{i,s}^{w}$ represents the percentage of the WT's generated active power.

### 3.2 Modelling of Solar irradiance

The solar irradiance modelling is done by using Beta PDF which is described as follows:

$$PDF(s) = \begin{cases} \dfrac{\Gamma(\alpha+\beta)}{\Gamma(\alpha)+\Gamma(\beta)} \times s^{\alpha-1} \times (1-s)^{\beta-1}, & 0 \le s \le 1, 0 \le \alpha, \beta \\ 0 & else \end{cases} \tag{4}$$

where $s$ is the solar irradiance (kW/m$^2$). $\alpha$ and $\beta$ are the parameters of Beta PDF which are derived as follows:

$$\beta = (1-\mu) \times \left( \frac{\mu \times (1-\mu)}{\sigma^2} - 1 \right) \tag{5}$$

$$\alpha = \frac{\mu \times \beta}{1-\mu} \tag{6}$$

where $\mu$ is the mean and $\sigma$ is the standard deviation of the random variable. The output power of PV is calculated with the help of Eqs. 7 and 8 respectively, the solar irradiance and the cell temperature as follow [31, 32]:

$$P_{pv} = P_{STC} \left\{ \frac{G}{1000} \left[ 1 + \delta \left( T_{cell} - 25 \right) \right] \right\} \tag{7}$$

$$T_{cell} = T_{amb} + \left( \frac{NOCT - 20}{800} \right) G \tag{8}$$

where $P_{pv}$ represents the PV output power in MW, $P_{STC}$ represents the power under standard test condition in MW, $\delta$ represents the power- temperature coefficient in (%/°C), $T_{cell}$ represents the cell temperature in °C, $T_{amb}$ represents the ambient temperature in °C, $NOCT$ are the national operating cell temperature conditions in *°C*, *G* is the solar irradiance in (W/m$^2$).

### 3.3 Load demand uncertainty modeling

To model load demands at each bus, Normal PDF is used. The normal distribution PDF for uncertain load $l$ is [33-34]:

$$PDF(l) = \frac{1}{\sigma_l \sqrt{2\pi}} \times \exp\left[ -\left( \frac{(l-\mu_l)^2}{2\sigma_l^2} \right) \right] \tag{9}$$

The genetic algorithm (GA) and support vector machine (SVM) based load forecasting uses point forecasts that does not estimates the full distribution of the future values while probabilistic forecasts provides the full distribution of the possible future values in such a way that it quantifies the uncertainties in the forecasts. Monte Carlo simulation and analytical state enumeration are the two existing techniques for DG system reliability assessment. The existing studies considered that all uncertainties related to DGs can be expressed by random variables X, described in terms of probability density function (PDF), f(x) [35].

### 3.4 Modelling approach

To model the uncertainties related to wind speed, solar irradiance and load demand, hourly data for one year (8760 h) consisting of load demand, wind speed, solar irradiance and price must be known. The following steps describes the methodology for uncertainty modeling.

Step-1: The whole data is divided into four seasons [summer (June-August), spring (September-November) winter (December-February) autumn (March-May) 2190 h each season]. A factorized data is obtained by dividing data into peak load demand, wind speed and solar irradiation.

Step-2: The demand curve is built by arranging daily historical demand data for 8760 h in descending order while keeping the hourly correlation between demand, wind and PV production. The ordered demand curve shows zones where high values have strong impact on NSW and consequently on network investment.

Step-3: The wind speed and solar irradiation curves are also built by arranging data form higher to lower value in each zone block. A cumulative distribution function is calculated for each time zone which is then divided into levels or segments, high, medium and low. The formulation of levels is similar for load demand, wind speed and solar irradiation.

Step-4: For each demand block, all combinations of demand, wind power factor and PV power factor levels are considered. Each combination is assigned a probability within the demand block equal to the probability of the demand factor level times the probability of the wind power factor and the PV power factor levels

Step-5: The formulation of scenarios is done for time blocks through the combination of the different levels of the data. Each load level $ll$ consist of a scenario $s$ that contains average demand factor $\mu_{ll,s}^{d}$, maximum wind power level $\mu_{ll,s}^{wind}$and PV power level $\mu_{ll,s}^{pv}$. For the present case study there are 108 scenarios in total obtained by multiplying 4 demand blocks, 3 factor levels for demand, 3 factor levels for wind power and 3 levels for PV power.

Fig.3 shows scenario-tree associated to each single considered variable (demand, wind and PV irradiation). The scenario tree represents the dynamics of the random parameters and the non-anticipatively of the decisions. In this modeling, it is assumed that there are $n$ number of probable future scenarios $s$ where each scenario represents relevant source of uncertainty.

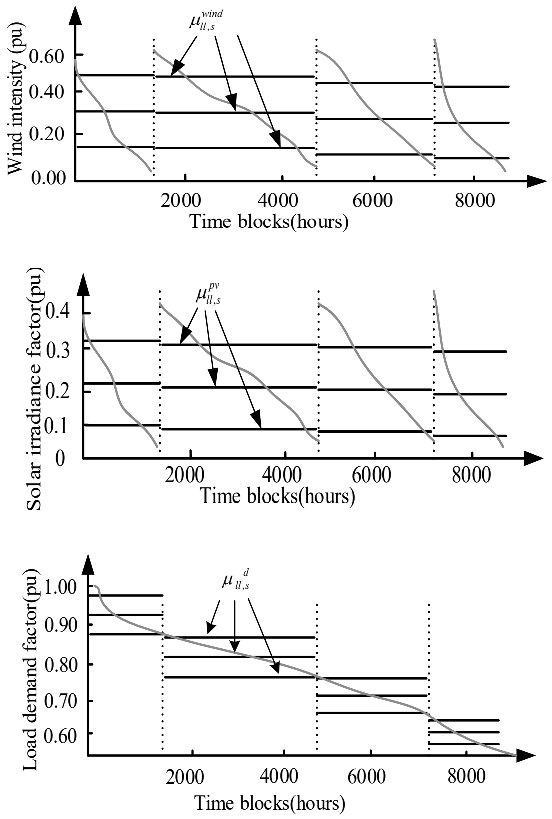


***Fig. 2.** Load, wind, and irradiation curves*

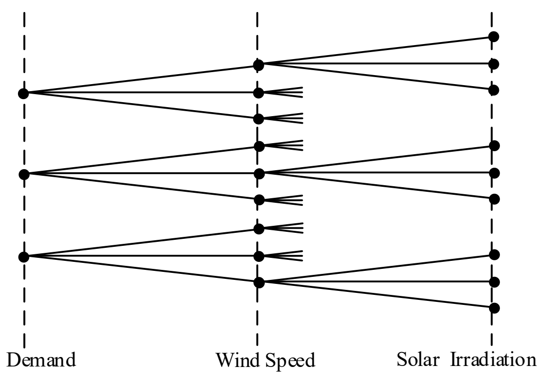


***Fig. 3** Scenario tree*

## 4. Planning of hybrid AC-DC microgrid

In this proposed hybrid AC-DC microgrid design, renewable-based distributed generators (DGs), controllable DGs, DC and AC loads are connected through separate DC and AC links. An operation model of hybrid microgrid is proposed in which mixed integer nonlinear model is suggested to balance the generation and load taking into account the interconnection of DC and AC subgrids for maximizing the social welfare. The efficiency of the proposed model is established through the simulation studies on a test hybrid AC-DC microgrid.

*A) Net social welfare*: The objective of HMG planning problem is to maximize the net social welfare (NSW) (10). It jointly maximises the consumers' benefits and minimises the total planning cost (13). The total planning cost consists of investment cost (IC) of all DGs and converters, operation and maintenance cost (OMC) of all DGs as well as the power exchange with utility grid. The cost for one planning year is the sum of IC and OMC.

$$\begin{aligned}\text{Maximise SW} = (&\sum_{h=1}^{NB}\sum_{s=1}^{NS}\sum_{y=1}^{NY} c^{LAC}_{h,s,y}P^{LAC}_{h,s,y} + \sum_{h=1}^{NB}\sum_{s=1}^{NS}\sum_{y=1}^{NY} c^{LDC}_{h,s,y}P^{LDC}_{h,s,y}) - \\ &(\sum_{s=1}^{NS}\sum_{y=1}^{NY} c_{slk,s,y}P_{slk,s,y} + \sum_{h=1}^{NB}\sum_{s=1}^{NS}\sum_{y=1}^{NY} c^{WIND}_{h,s,y}P^{WIND}_{h,s,y} + \\ &\sum_{h=1}^{NB}\sum_{s=1}^{NS}\sum_{y=1}^{NY} c^{PV}_{h,s,y}P^{PV}_{h,s,y} + \sum_{s=1}^{NS}\sum_{y=1}^{NY} C^{PG}_{s,y})\end{aligned} \quad (10)$$

where $C^{PG}$= RR(IC + OMC) (11)

Note that capital recovery rate RR is present in cost function, calculated as

$$RR = \frac{1}{(1+r)^{t+1}} \quad (12)$$

where $t$ is the planning horizon and $r$ is the discount rate and the planning horizon is considered to be for ten years period.

$$\begin{aligned}IC = &\sum_{a=1}^{NG}\sum_{h=1}^{NB}\sum_{s=1}^{NS}\sum_{y=1}^{NY} CC_a P^{MAX}_{h,s,y} f_{ha} + CR\sum_{a=1}^{NG}\sum_{h=1}^{NB}\sum_{s=1}^{NS}\sum_{y=1}^{NY} P^{WIND}_{h,s,y} f_{ha} d_h + \\ &CI\sum_{a=1}^{NG}\sum_{h=1}^{NB}\sum_{s=1}^{NS}\sum_{y=1}^{NY} P^{PV}_{h,s,y} f_{ha}(1-d_h) + \sum_{h=1}^{NB}\sum_{s=1}^{NS}\sum_{y=1}^{NY}\{CIP^{LAC}_{h,s,y} d_h + \\ &CRP^{LDC}_{h,s,y}(1-d_h)\} + CIP^{LIMIT}W\end{aligned} \quad (13)$$

$$\begin{aligned}OMC = &\sum_{h=1}^{NB}\sum_{s=1}^{NS}\sum_{y=1}^{NY} CostAC_{h,s,y} + \sum_{h=1}^{NB}\sum_{s=1}^{NS}\sum_{y=1}^{NY} CostDC_{h,s,y} + \\ &\sum_{h=1}^{NB}\sum_{s=1}^{NS}\sum_{y=1}^{NY} \rho_{h,s,y} P^{Fexch}_{h,s,y}\end{aligned} \quad (14)$$

where $CostAC = C_{AC} \times P^{Gwind}$ and $CostDC = C_{DC} \times P^{Gpv}$ (15)

*B) Constraints*: The objective function is subject to following investment and operation constraints.

1) *DER Connectivity:* Each DER is connected to only one feeder.

$$\sum_{a=1}^{NG} f_{ha} \le 1 \quad (16)$$

2) *Installed capacity:* Installed capacity is greater than peak load demand is shown in Eq. (17).

$$\sum_{a=1}^{NG} P^{LAC}_{h,s,y} + \sum_{a=1}^{NG} P^{LDC}_{h,s,y} \le \sum_{h=1}^{NB}\sum_{a=1}^{NG}\{P^{WIND}_{h,s,y} + P^{PV}_{h,s,y}\} f_{ha} \quad (17)$$

3) *Power balance:* Equation (8) represents the power balance equation which has to be satisfied at each bus.

$$\begin{aligned}&(\sum_{a=1}^{NG} P^{LAC}_{h,s,y} \times ((d_h / EI) + (1-d_h)) + \sum_{a=1}^{NG} P^{LDC}_{h,s,y}(d_h + (1-d_h)/ER) \\ &= \sum_{a=1}^{NG} P^{WIND}_{h,s,y} \times (ER \times d_h + (1-d_h)) + \sum_{a=1}^{NG} P^{PV}_{h,s,y}(d_h + \\ &EI(1-d_h)) + P^{Fexch}_{h,s,y}(ER \times d_h + (1-d_h))\end{aligned} \quad (18)$$

4) *AC Power generation limit:* Power generated by AC based DGs is limited by their installed capacity is shown in Eq. (19).

$$0 \le P^{WIND}_{h,s,y} \le P^{MAX}_{h,s,y} \quad (19)$$

5) *DC Power generation limit:* Power generated by DC based DGs is limited by their installed capacity.

$$0 \le P_{h,s,y}^{PV} \le P_{h,s,y}^{MAX} \quad (20)$$

6) *Maximum Power:* Total installed capacity of all DGs is equal to sum of total generated power.

$$P_{h,s,y}^{MAX} = \sum_{a=1}^{NG} P_{h,s,y}^{WIND} + P_{h,s,y}^{PV} \quad (21)$$

7) *Voltage limits:* Voltage at each bus is limited by the boundary values.

$$V_h^{\min} \le V_h \le V_h^{\max} \quad (22)$$

where $h$ is the number of AC and DC buses, $a$ is set of generators buses. It is assumed that WTs are installed at buses 2, 3, 6 and 8 while PVs are installed at buses 16, 17, 20 and 22. It should be noted that buses 1 to 14 belong to ac subgrid and buses 15 to 28 to dc subgrid. . $c_{h,s,y}^{LAC}$ and $c_{h,s,y}^{LDC}$ are the bid prices for AC and DC load demands, respectively at bus $h$, scenario $s$ and year $y$. $P_{h,s,y}^{LAC}$ and $P_{h,s,y}^{LDC}$ are the active power for ac and dc load demand respectively at bus $h$, scenario $s$ and year $y$. The investment cost (13) comprises of DG investment cost (first term) and the cost of converters (rest of the terms). The investment cost of DG is calculated as installed power capacity $P_{h,s,y}^{MAX}$ times the capital cost $CC_a$ of distributed energy resources (DER). The $P_{h,s,y}^{MAX}$ will be determined at the time of planning. A binary decision variable $f_{ha}$ is also introduced in the investment cost of DG. The $f_{ha}$ has two functionalities, first it gives information that DG is installed and secondly it also gives information about the bus to which DG is connected. If $f_{ha}$ is 1 in planning, this means DG $a$ will be installed and will be connected to bus h. The next four terms in the investment cost are modelled using binary decision variable $d_h$ that determine the type of bus, i.e. AC or DC. If $d_h$ is 1 in planning it means it is dc feeder and for ac feeder $d_h$ is set to zero. If $d_h$ is zero it means feeder is ac and an additional cost of inverter (CI) will be added if dc-based DG is to be used in planning to connect with ac grid. Similarly if $d_h$ is set to 1 in the planning problem then feeder is said to be dc and an additional cost of rectifier (CR) will be added if AC DG is to be used to connect with dc feeder. The second and third terms in (13) represents the cost of converter and inverter on the generation side, respectively. While fourth and fifth terms in (13) represent the cost of converter and inverter on the load side. The last term in (13) represents the cost of inverter required to connect dc feeder with utility grid. A binary decision variable $W$ is also introduced in last term. If $W$ is set to zero it means there is no dc feeder but if $W$ is set to 1 it means at least one feeder is dc. $P^{Limit}$ is the flow limit between the microgrid and the utility grid.

The operation and maintenance cost (14) includes three parts, the first and second terms represents the generation cost of DGs while third term represents the cost of energy purchased from the grid. The generation cost of DGs is the sum of amount of energy produced by each DG (CostAC/CostDC) times the price of its generation $C_{h,s,y}$. The third term in (14) represents the total energy exchange with the grid times the market price at the time of exchange of power. The total energy exchange with the grid ($P_M$) is equal to the sum of energy exchange at each feeder ( $P_{h,s,y}^{Fexch}$ ).

## 5. Hybrid microgrid electricity market model

A hybrid AC-DC microgrid electricity market model is proposed in this section. The hybrid microgrid market operator (HMMO) is a platform that enables market activities for end user customers, controls the operational facilities and it buys active power from bilateral contracts or through the pool. Dispatchable loads (DLs), WTs and PVs sends offers and bids prices of active power in form of blocks to the hybrid microgrid market (HMM) every hour. To maximize the NSW, the HMMO combines offers and bids prices.

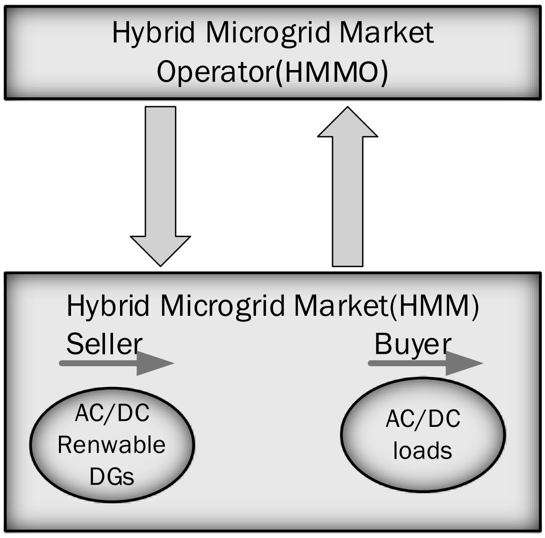


***Fig. 4*** *Proposed Hybrid Microgrid Electricity Market Structure*

Two major responsibilities of the HMMO within this structure are:

1) To receive demand bids from HMM and offer an aggregated bid to the wholesale energy market.
2) From the wholesale energy market, it will receive schedule of WTs, PVs and DLs according to the market prices one day ahead. WTs, PVs and DLs will provide offer and bid prices and active power quantity information for every 24-hour trading period one day ahead.

HMM would submit their bids to the HMMO and later be notified by HMMO on the amount of awarded power. The amount of power exchange with distribution network is assigned by HMMO, hence it is known to the HMMO in advance which minimizes uncertainties caused by the HMM. Once the power exchange with the utility grid and HMM is known in advance for the 24 hours of the next day, the HMM would solve a market-based scheduling problem to optimize the scheduling of its DGs and loads.

## 6. Case study

The effectiveness of the proposed method is verified through the simulation studies on a 28-bus real hybrid AC-DC microgrid based in , Pakistan [36]. The single-line diagram of a 28-bus real hybrid AC-DC microgrid is shown in Fig. 5. It constitutes of an AC subgrid with conventional DG sources, DC subgrid with DC sources and an interlinking converter (IC) which links the two subgrids together. Each of the subgrids includes their individual loads. The hybrid AC-DC microgrid is connected to the utility grid during normal grid operation. The proposed hybrid AC-DC microgrid reduces multiple power conversion processes in an individual AC or DC grid. The market-based optimal power flow is used to maximize the NSW in order to find the optimal capacity of WTs and PVs. The load increment is assumed to be 3% yearly over the planning horizon. In this paper, it is assumed that buses 2, 3, 6 and 8 are four possible locations for WTs to be installed at AC subgrid and 8, 15, 16, 17, 20 and 22 are five possible locations for PVs to be installed at DC subgrid, respectively. It is notable that the selection of possible locations of WTs and PVs relies on non-technical factors such as legal requirements, space/land availability and other amenities. It is assumed that four 660kW WTs at buses 2, 3, 6 and 8 while five 440kW PVs at buses 15, 16, 17 18 and 20 are installed. WTs and PVs can be allocated at AC and DC buses, respectively. For each scenario, this is represented by three blocks in the WT's and PV's offer with the following price presented in Tables 2 and 3 respectively.

**Table 2** Active power bid prices for the WT's

| Bus No. | Active power bid price list for WT's Blocks (MW@£/MWh) | | |
|---|---|---|---|
| | $b_1$ | $b_2$ | b3 |
| 2 | 2.51@280 | 1.90@270 | 1.46@250 |
| 3 | 1.10@270 | 0.70@260 | 0.15@250 |
| 4 | 0.02@260 | 0.03@250 | 0.01@240 |
| 5 | 1.18@250 | 1.12@240 | 1.15@230 |
| 6 | 01.9@240 | 0.61@240 | 0.32@230 |
| 7 | 0.91@250 | 0.59@230 | 0.49@230 |
| 9 | 0.21@240 | 0.52@220 | 0.29@220 |
| 10 | 1.41@240 | 0.89@210 | 0.42@220 |
| 11 | 1.50@230 | 0.90@210 | 0.49@210 |
| 12 | 0.45@220 | 0.21@200 | 0.34@190 |
| 13 | 0.69@220 | 0.21@190 | 0.22@180 |
| 14 | 0.35@190 | 0.15@180 | 0.17@170 |

**Table 3** Active power bid prices for the PV's

| Bus No. | Active power bid price list for PV's Blocks (MW@£/MWh) | | |
|---|---|---|---|
| | b1 | b2 | b3 |
| 15 | 0.81@240 | 1.60@230 | 1.16@220 |
| 16 | 1.13@240 | 0.70@230 | 0.15@210 |
| 17 | 0.92@230 | 0.03@220 | 0.01@210 |
| 18 | 0.78@220 | 6.12@220 | 3.15@200 |
| 19 | 1.90@220 | 0.61@220 | 0.26@200 |
| 20 | 0.91@210 | 0.59@220 | 0.51@190 |
| 21 | 0.21@200 | 0.20@210 | 0.19@190 |
| 22 | 1.41@200 | 0.89@210 | 0.52@180 |
| 23 | 1.50@190 | 0.90@200 | 0.49@180 |
| 24 | 0.45@190 | 0.21@200 | 0.14@170 |
| 25 | 0.69@190 | 0.21@190 | 0.31@170 |
| 26 | 0.35@190 | 0.15@180 | 0.09@160 |
| 27 | 0.35@180 | 0.35@170 | 0.39@160 |
| 28 | 0.35@180 | 0.35@170 | 0.35@160 |

Assuming a load growth of 3% for each year of the planning horizon, the dispatched wind active power increases proportionally to the load demand growth. This is mainly due to the proportional relation between wind generation and the size of the blocks in the WT's offer and to the assumption of a proportional load increase at all buses that alleviates voltage and thermal constraints as shown in Fig. 6, 7, 8 and 9 respectively. The total yearly active power dispatched by WTs at all candidate buses is shown in Fig. 10. The dispatched PV active power at each candidate bus also increases proportionally to the load demand growth as the 3% load growth for each year is also assumed for each year of the planning horizon as shown in Fig. 11. As expected, due to the WTs and PVs installations, the NSW also increases proportionally to load demand wind and solar generation during each year of the planning horizon, as shown in Fig. 12. In Fig.13, the comparison of the social welfare for first twenty scenarios for year 1 and year 10 is shown. It can be seen in that social welfare increases in each scenario in the last year compared to one in the first year.

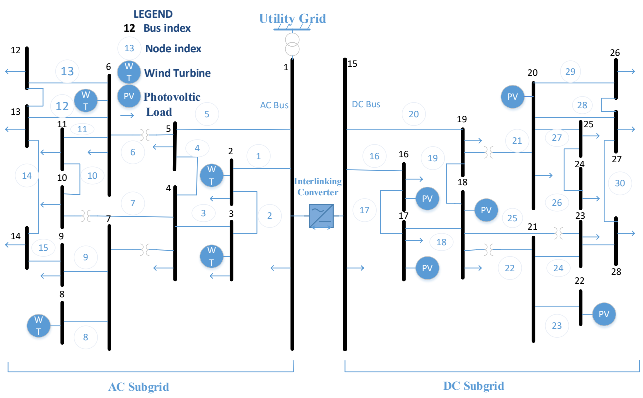


***Fig.5.*** *Single-line diagram of real Hybrid ac-dc microgrid*

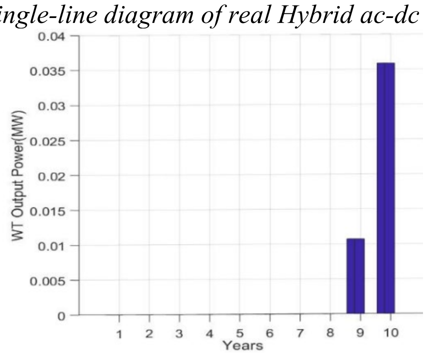


***Fig.6.*** *Total yearly dispatched Wind active power at bus 2*

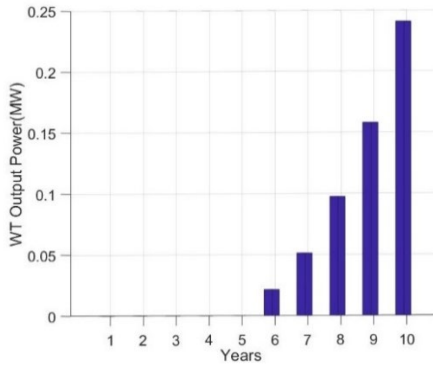


***Fig.7.*** *Total yearly dispatched Wind active power at bus 3*

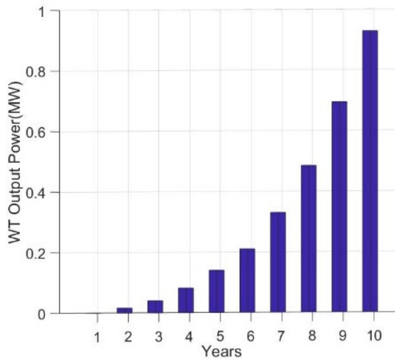


***Fig.8.*** *Total yearly dispatched Wind active power at bus 6*

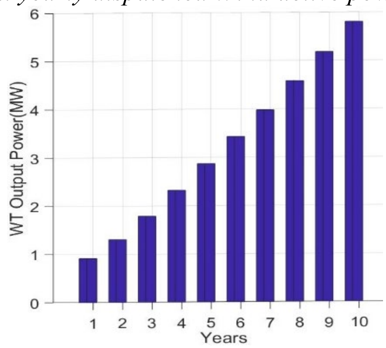


***Fig.9.*** *Total yearly dispatched Wind active power at bus 8*

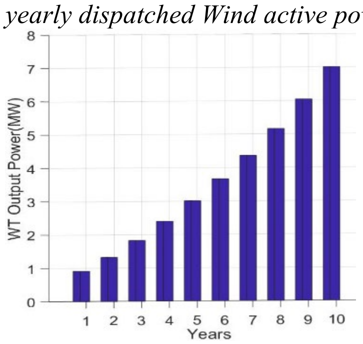


***Fig.10.*** *Total yearly dispatched Wind active power*

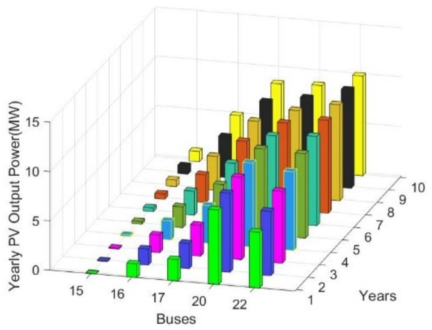


***Fig.11.*** *Total yearly dispatched PV active power*

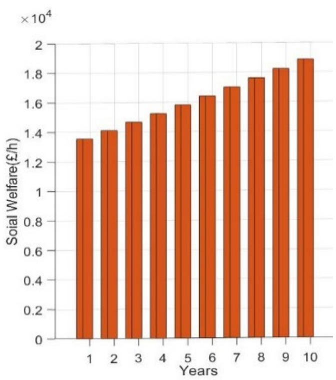


***Fig.12***. *Total Net Social Welfare over the planning horizon*

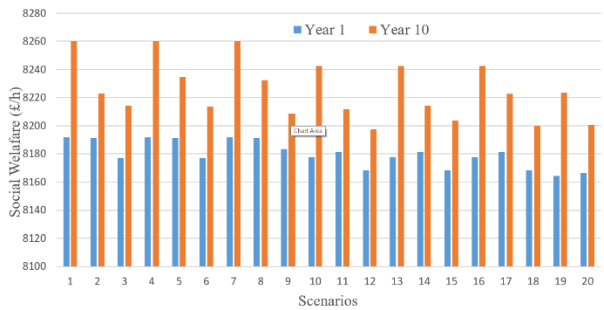


***Fig.13***. *Social welfare for 20 scenarios in year 1 and year 10 of the planning horizon*

## 7. Conclusion

In this paper, a novel stochastic approach for planning and design of hybrid microgrids within a market environment was proposed. The method evaluates the amount of active power generated by WT and PV that can deliver to the load and the amount of active power injected or absorbed from the grid. Scenario based approach is used to model the uncertainty related to the wind speed, solar irradiation and load demand.

The proposed model numerical simulation proves the viability of hybrid AC-DC microgrid in supplying loads. The objective of hybrid AC-DC microgrid planning problem is to maximize NSW to simultaneously maximise consumers' payments and reduce total planning cost.

The proposed configuration will help hybrid AC-DC microgrid planners to estimate planning cost with flexibility to consider any type of load ac/dc and the type of DERs. Different components of hybrid AC-DC microgrid were explained, followed by developing the hybrid AC-DC microgrid planning model with the objective of determining the optimal DERs generation mix and reduced planning cost.

Our future work is to develop a model for the network reinforcement and design of hybrid AC-DC microgrid. In this paper, for the sake of simplicity, AC based conventional DG sources are placed on AC subgrid and DC sources are placed on DC subgrid. However, we aim to develop the proposed formulation to be able to accommodate AC based conventional DG sources and DC sources on both AC and DC subgrids and in optimal locations. Authors are also working on active network management (ANM) schemes that includes coordinated voltage control (CVC) of on-load tap changers (OLTCs) and adaptive power factor control (PFC) which will offer a feasible solution for HMMO for optimal active management and optimal planning and operation of the HMG.

References

[1] Albadi, M.H. and El-Saadany, E.F., 2008. A summary of demand response in electricity markets. Electric power systems research, 78(11), pp.1989-1996.

[2] Omer, A.M., 2008. Energy, environment and sustainable development. Renewable and sustainable energy reviews, 12(9), pp.2265-2300.

[3] Act, C.C., 2008. Climate Change Act 2008. See http://www. legislation. gov. uk/ukpga/2008/27/contents (accessed 13/11/2013).

[4] Fais, B., Sabio, N. and Strachan, N., 2016. The critical role of the industrial sector in reaching long-term emission reduction, energy efficiency and renewable targets. Applied Energy, 162, pp.699-712.

[5] Hatziargyriou, N., Asano, H., Iravani, R. and Marnay, C., 2007. Microgrids. IEEE power and energy magazine, 5(4), pp.78-94.

[6] Piagi, P. and Lasseter, R.H., 2006, June. Autonomous control of microgrids. In Power Engineering Society General Meeting, 2006. IEEE (pp. 8-pp). IEEE.

[7] Fang, X., Misra, S., Xue, G. and Yang, D., 2012. Smart grid—The new and improved power grid: A survey. IEEE communications surveys & tutorials, 14(4), pp.944-980.

[8] Justo, J.J., Mwasilu, F., Lee, J. and Jung, J.W., 2013. AC-microgrids versus DC-microgrids with distributed energy resources: A review. Renewable and Sustainable Energy Reviews, 24, pp.387-405.

[9] Lotfi, H. and Khodaei, A., 2017. AC versus DC microgrid planning. IEEE Transactions on Smart Grid, 8(1), pp.296-304.

[10] Basak, P., Chowdhury, S., nee Dey, S.H. and Chowdhury, S.P., 2012. A literature review on integration of distributed energy resources in the perspective of control, protection and stability of microgrid. Renewable and Sustainable Energy Reviews, 16(8), pp.5545-5556.

[11] Planas, E., Andreu, J., Gárate, J.I., de Alegría, I.M. and Ibarra, E., 2015. AC and DC technology in microgrids: A review. Renewable and Sustainable Energy Reviews, 43, pp.726-749.

[12] Yazdanian, M. and Mehrizi-Sani, A., 2014. Distributed control techniques in microgrids. IEEE Transactions on Smart Grid, 5(6), pp.2901-2909.

[13] Prodan, I., Zio, E. and Stoican, F., 2015. Fault tolerant predictive control design for reliable microgrid energy management under uncertainties. Energy, 91, pp.20-34.

[14] Radwan, A.A.A. and Mohamed, Y.A.R.I., 2012. Assessment and mitigation of interaction dynamics in hybrid AC/DC distribution generation systems. IEEE Transactions on Smart Grid, 3(3), pp.1382-1393.

[15] Khodaei, A., Bahramirad, S. and Shahidehpour, M., 2015. Microgrid planning under uncertainty. IEEE Trans. Power Syst, 30(5), pp.2417-2425.

[16] Liu, X., Wang, P. and Loh, P.C., 2011. A Hybrid AC/DC Microgrid and Its Coordination Control. IEEE Trans. Smart Grid, 2(2), pp.278-286.

[17] Hatziargyriou, N., Asano, H., Iravani, R. and Marnay, C., 2007. Microgrids. IEEE power and energy magazine, 5(4), pp.78-94.

[18] Rahman, M.S., Hossain, M.J. and Lu, J., 2016. Coordinated control of three-phase AC and DC type EV–ESSs for efficient hybrid microgrid operations. Energy conversion and management, 122, pp.488-503.

[19] Gu, W., Wu, Z., Bo, R., Liu, W., Zhou, G., Chen, W. and Wu, Z., 2014. Modeling, planning and optimal energy management of combined cooling, heating and power microgrid: A review. International Journal of Electrical Power & Energy Systems, 54, pp.26-37.

[20] Tan, X., Li, Q. and Wang, H., 2013. Advances and trends of energy storage technology in Microgrid. International Journal of Electrical Power & Energy Systems, 44(1), pp.179-191.

[21] Eghtedarpour, N. and Farjah, E., 2014. Power control and management in a hybrid AC/DC microgrid. IEEE transactions on smart grid, 5(3), pp.1494-1505.

[22] Lotfi, H. and Khodaei, A., 2017. Hybrid AC/DC microgrid planning. Energy, 118, pp.37-46.

[23] Mahmud, N. and Zahedi, A., 2016. Review of control strategies for voltage regulation of the smart distribution network with high penetration of renewable distributed generation. Renewable and Sustainable Energy Reviews, 64, pp.582-595.

[24] Zubo, R.H., Mokryani, G. and Abd-Alhameed, R., 2018. Optimal operation of distribution networks with high penetration of wind and solar power within a joint active and reactive distribution market environment. Applied Energy, 220, pp.713-722.

[25] A. N. Celik, "A statistical analysis of wind power density based on the Weibull and Rayleigh models at the southern region of Turkey," *Renewable energy,* vol. 29, pp. 593-604, 2004.

[26] [26] S. S. Reddy, A. Abhyankar, and P. Bijwe, "Market clearing for a wind-thermal power system incorporating wind generation and load forecast uncertainties," in *Power and Energy Society General Meeting, 2012 IEEE*, 2012, pp. 1-8.

[27] [27] G. Mokryani, "Active distribution networks operation within a distribution market environment," in *Sustainable Development in Energy Systems*, ed: Springer, 2017, pp. 107-118.

[28] S. S. Reddy, B. Panigrahi, R. Kundu, R. Mukherjee, and S. Debchoudhury, "Energy and spinning reserve scheduling for a wind-thermal power system using CMA-ES with mean learning technique," *International Journal of Electrical Power & Energy Systems,* vol. 53, pp. 113-122, 2013.

[29] [30] S. S. Reddy and J. A. Momoh, "Realistic and transparent optimum scheduling strategy for hybrid power system," *IEEE Transactions on Smart Grid,* vol. 6, pp. 3114-3125, 2015.

[30] [31] G. Mokryani, A. Majumdar, and B. C. Pal, "Probabilistic method for the operation of three-phase unbalanced active distribution networks," *IET Renewable Power Generation,* vol. 10, pp. 944-954, 2016.

[31] S. Montoya-Bueno, J. Muñoz-Hernández, and J. Contreras, "Uncertainty management of renewable distributed generation," *Journal of Cleaner Production,* vol. 138, pp. 103-118, 2016.

[32] J. Widén, "Correlations between large-scale solar and wind power in a future scenario for Sweden," *IEEE transactions on sustainable energy,* vol. 2, pp. 177-184, 2011.

[33] S. S. Reddy, P. Bijwe, and A. R. Abhyankar, "Joint energy and spinning reserve market clearing incorporating wind power and load forecast uncertainties," IEEE Systems Journal, vol. 9, pp. 152-164, 2015.

[34] S. S. Reddy, P. Bijwe, and A. R. Abhyankar, "Optimal posturing in day-ahead market clearing for uncertainties considering anticipated real-time adjustment costs," IEEE Systems Journal, vol. 9, pp. 177-190, 2015.

[35] Li, Y. and Zio, E., 2012. Uncertainty analysis of the adequacy assessment model of a distributed generation system. Renewable Energy, 41, pp.235-244.

[36] http://cuiatd.edu.pk/secure/researchgroups/COMSATSResearchProjects.aspx?deptID=3&groupID=3&groupName=Electrical%20Power%20and%20Control%20Systems%20(EPCS)%20Research%20Group